International Pharmacy Acta. 2019;2(1):e1
Original Research Article
OPEN ACCESS
ISSN: 2645-3266

Mice fetus liver tissue spectroscopic alterations following concomitant administration of Metronidazole & Miconazole

Azadeh Ashtarinezhad[a], Ataollah Panahyab[b], Farshad H.Shirazi[c, d]*

a. Department of Occupational Health, School of Public Health, Iran University of Medical Sciences, Tehran, Iran.
b. Young Researchers and Elite club, Central Tehran Branch, Islamic Azad University, Tehran, Iran.
c. Department of Toxicology, School of Pharmacy, Shahid Beheshti University of Medical Sciences, Tehran, Iran.
d. Pharmaceutical Sciences Research Center, Shahid Beheshti University of Medical Sciences, Tehran, Iran.

Article Info:
Received: February 2019
Accepted: April 2019
Published online:
May 2019

*** Corresponding Author:**
Farshad H.Shirazi
Email: f.shirazi@sbmu.ac.ir

ABSTRACT:
Introduction: Metronidazole (MET) and Miconazole (MIC) are antiprotozoal and imidazole antifungal agents, respectively. The aim of this study was to assess the usefulness of Fourier Transform Infrared micro-spectroscopy (FTIR-MSP) for discriminating and detecting spectral changes of mouse fetus liver tissue after mother's exposure to concomitant use of MET and MIC. **Methods and Results:** The control group received only normal diet and the exposure groups received MET, MIC, and concomitant MET and MIC. The pregnant mice were anesthetized and their fetuses were surgically removed on gestation day 15. Fixative slides without any staining were put on KBr disc with a 1mm thick for IR micro spectroscopy. All information obtained from the spectra were analyzed using routine FTIR software. Based on our results, MET and MIC, alone and in combination together, have created some changes in the mice fetus liver biomolecules. **Conclusion:** FTIR biospectroscopy application in teratology is very challenging, but it has been accepted as a reliable technique; however, it is necessary to do more investigations.

Keywords: FTIR- MSP; Metronidazole; Miconazole; Mice fetus liver tissue.

Please Cite this article as: Ashtarinezhad A, Panahyab A, H.Shirazi F. Mice fetus liver tissue spectroscopic alterations following concomitant administration of Metronidazole & Miconazole. Int. Pharm. Acta. 2019;2(1):e1
DOI: https://doi.org/10.22037/ipa.v2i1.22244

1. Introduction

Metronidazole (MET) (a nitro imidazole) is an antiprotozoal and antibacterial medication, selectively absorbed by anaerobic bacteria and sensitive protozoa [1-4]. Miconazole (MIC) is an imidazole antifungal agent, usually applied topically to the skin or mucous membranes to cure fungal infections [5-7]. MET and MIC are used for fungal and volvo vaginal infections like candidiasis, bacterial vaginitis, and trichomonas vaginitis. Concomitant use of MET and MIC during pregnancy , especially at the organogenesis period, causes polydactylyl and syndactylyl in the upper organs, defective skeletal system, cleft palate, rib deformity, skull deformation, and so on. [7-19].

Fourier Transform Infrared micro-spectroscopy (FTIR-MSP) is a powerful technique to provide sensitive and accurate measurement of biochemical changes in the biological cells and tissues. This approach provides structural information of biological molecules, such as proteins, nucleic acids, carbohydrates, and lipids, allowing detection, identification, and quantification of changes in these biomolecules. This technique is very rapid, non-destructive, and non-invasive for the sample, and requires low sample volume. This technique has also been used for the characterization and discrimination of diseased tissues from normal ones, particularly in cancer detection. Some of the most investigated tissues in this regard are cervix, lung,

breast, skin, gastrointestinal, brain, lymphoid, prostate, and colon. That is why the clinical applications of spectroscopic data have attracted attention of both the clinicians and the basic sciences researchers [20-32].
The ability of FTIR spectroscopy to determine the drugs induced abnormalities in fetus tissues has been shown in authors' previous paper [31]. The present study aimed to determine the teratogenicity of MET and MIC in combination together by FTIR-MSP.

2. Materials & Methods

2.1. Preparation of the sample for FTIR-MSP

Adult mice (10-12 weeks), weighed 20g, were purchased from Pasture institute, Iran. The laboratory NMRI mice were maintained under standard conditions (light period of 12 h/day, temperature (22°C), relative humidity (45%), and ventilation (15 air changes/hour)) with access to water and libitum, and all the experiments were carried out based on a protocol approved by local animal care ethical committee. MET and MIC were purchased from Daroopakhsh Pharmaceutical Company, Iran. After checking the vaginal plaque to identify the pregnant mice, they divided into four groups of ten animals eachand treated according to the method previously reported [33-36]: 1) the control group received only normal diet, group MET received Metronidazole (60 mg/kg), group MIC received Miconazole (60 mg/kg), and the last group (MET plus MIC) received 60 mg/kg of Metronidazole plus 60 mg/kg of Miconazole on the 9th day of gestation intraperitoneally. The fetuses were assessed on gestation day 15 for morphological and histological changes according to the reference [37], and then embedded in paraffin after fixation with Bouinn's solution. Histological sections were prepared [29] by microtome instrument (10 µm), stained with haematoxylin and eosin (HE)[38], and then examined under light microscopy for signs of fetal abnormalities. Slides without any staining were put on KBr disc with a 1mm thick for IR micro spectroscopy.

2.2. FTIR-MSP

FTIR measurements were carried out using WQF-510 Fourier transform spectrometer (Rayleigh Optics, China) with a KBr beam splitter, equipped with a detector of DLaTGS (deuterated, L-alanine doped triglycine sulfate), IR microscope of µMAX (PIKE Technologies, USA), and a KBr disc (13mm x 3mm), in the absorbance mode and all the spectra were scanned in the mid-IR range of 4000 to 400 cm^{-1} (resolution of 4 cm^{-1}).

2.3. Data processing and analysis

100 scans were co-added for each spectrum from several sites of the mouse fetus liver tissues sections to reach high signal to noise ratio (SNR). All information, obtained from the spectra, was analyzed using routine FTIR software. The average spectrum was calculated by averaging repetitive spectra (30 spectra per sample) and then employed for various mathematical manipulations. Baseline correction and normalization to the band at 1545 cm^{-1} (amide II peak) as a reference for uniformity, were done for all the spectra [26] and second order derivatives were also calculated for specific regions.

2.4. Statistics

The tissue pathologic evaluated data from the treated fetus weight and the C-R length were analyzed using Graphpad Prism© software. The findings of the MET, MIC, and MET plus MIC mouse fetus weight and C-R were analyzed using one-way variances analysis, followed by Tukey test ($p<0.01$). These findings were expressed as Mean±SD. One-way analysis of variances, followed by Tukey test ($p<0.01$), were done on FTIR spectral information using Origin Pro software (Version 8.5.1) for checking the possibility of significant difference between the mentioned groups.

3. Results and discussion

3.1. Morphological studies

Photomicrographs were prepared from the control, MET, MIC, and MET plus MIC treated tissue sections (Figure 1) and investigated by light microscope. Umbilical hernia, enlarged liver, and reducing the number of fetus were observed in MET plus MIC treated mouse fetus., There were some abnormalities in this group, such as brain developmental retardation, formation of heart out of mouse fetus body, deviation of the hands and feet, syndactylyl, hemoral, skull deformity, and short tail.

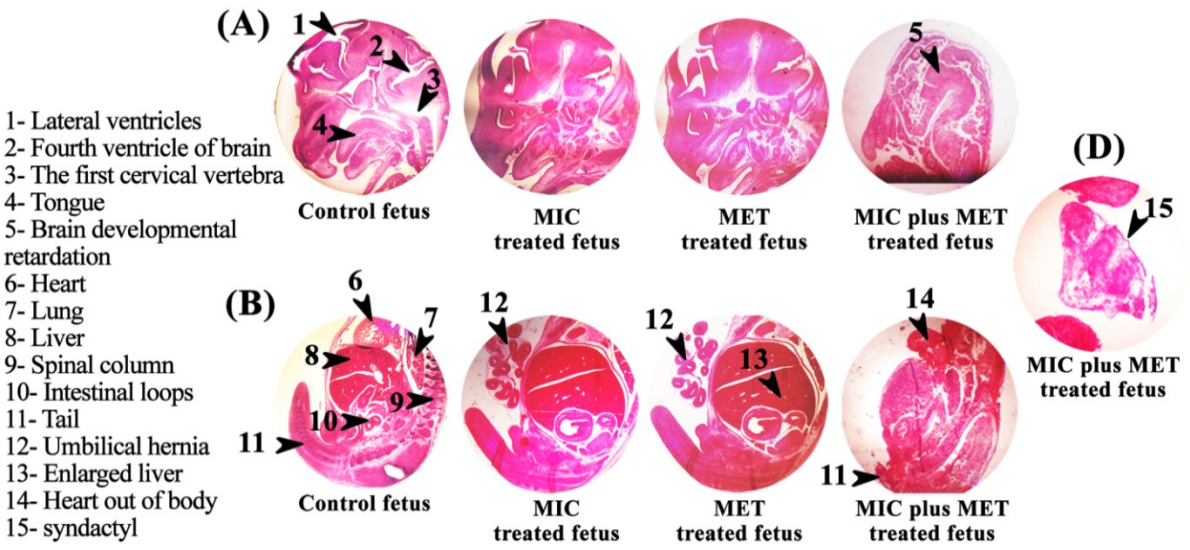

Figure 1. HE stained sections of the control, MET, MIC (Umbilical hernia, Enlarged liver) and MET plus MIC mouse fetus tissues (heart formation in out of body, Short tail, Syndactylyl , Brain developmental retardation).

The weight (Fig. 2A) and the C-R length (Fig. 2B) of MET plus MIC treated mouse fetus were less than the other groups and there were significant difference between them with $p<0.01$.

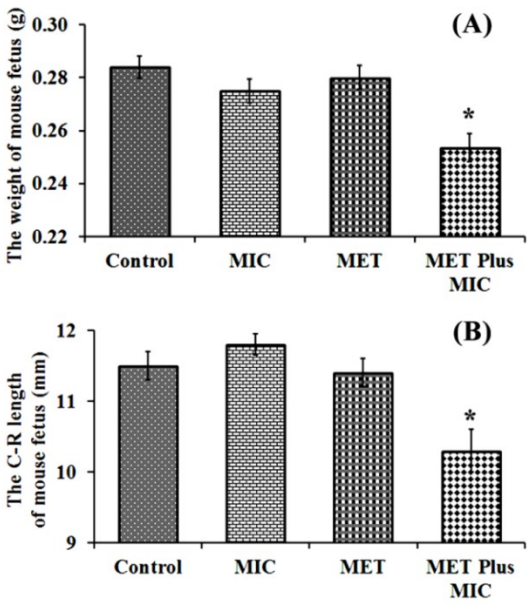

Figure 2. The weight of the mouse fetus (A), (control= 28.4gr; MET= 28.8 gr; MIC= 27.6gr; and MET plus MIC= 25.4gr); ($p< 0.01$). * Significant difference versus the other group weights. The C-R of the mouse fetus (B), (control=11.5mm; MET= 11.4mm; MIC= 11.8mm; and MET plus MIC= 10.3mm), ($p< 0.01$). * Significant difference versus the other groups C-R. MET= Metronidazole and MIC= Miconazole.

3.2. The drugs treated mouse fetus liver tissues (FTIR-MSP spectral characteristics)

Figure 4 and 5 reveal a band at 1146 cm^{-1}, due to the membrane-bound oligosaccharide C-OH bond, was disappeared in the MET treated fetus liver tissue, whereas it was present in the MIC treated and MET plus MIC treated fetus liver tissue. In the MIC treated and MET plus MIC treated fetus liver tissues, a band at 1107 cm^{-1},attributed to the ν (CO), ν (CC), and ring (polysaccharides, pectin) shifted, and also increased, and decreased, respectively, while it just reduced in fetus liver tissue, exposed to MET. A band at 1016 cm^{-1}, due to the ν (CO), ν (CC), δ (OCH), and ring (polysaccharides, pectin), was appeared in the MIC treated fetus liver tissue but it was not present in the MET treated and MET plus MIC treated fetus liver tissues. Intensity at 1232 cm^{-1} and 1029 cm^{-1}, due to the amid III and O-CH3 stretching of methoxy groups, respectively, decreased and shifted in the MET plus MIC treated fetus liver tissues, while it decreased without any shifting in the MET treated and MIC treated fetus liver tissues. A band at 1210 cm^{-1}, related to the $PO^{-}2$ asymmetric (phosphate I), was appeared in the MET treated fetus liver tissue. Intensity at 1729 cm^{-1}, ascribed to the absorption band of fatty acid

ester band, increased and shifted in the MET plus MIC treated fetus liver tissue. A band at 1717 cm^{-1}, due to the amid I, was disappeared in the MIC treated fetus liver tissue. Intensity at 1661 cm^{-1}, due to the amid I, increased and shifted in the MET plus MIC treated fetus liver tissue.

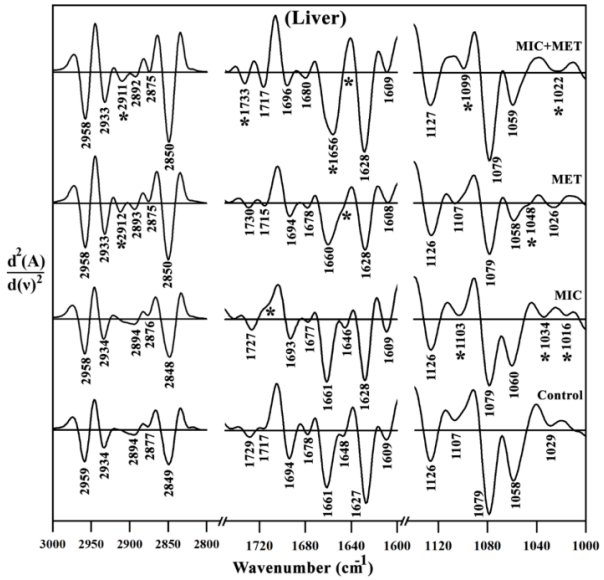

Figure 3. Mid-infrared spectra and the differential spectra (treated liver sections spectra-control sections spectra) of control and MET, MIC and MET plus MIC mice fetus liver tissue sections in the 1000–3500 cm^{-1} wavenumber region. Baseline correction and normalization were done for all the spectra with a reference to the band at 1545 cm^{-1} (amide II peak) for uniformity.

A band at 1648 cm^{-1}, related to the amid I, was present in the control and MIC treated fetus liver tissues, while it was disappeared in the MET treated and MET plus MIC treated fetus liver tissues. Intensity at 1593 cm^{-1}, attributed to the C=N, NH2 adenine, decreased and shifted in the MIC treated fetus liver tissue. The bands at 1569 cm^{-1} and 1534 cm^{-1}, owing to the amid II, were disappeared in the MET plus MIC treated fetus liver tissue, while there were present in the control, MET treated, and MIC treated fetus liver tissues. Intensity at 1549 cm^{-1}, related to the amid II, increased and shifted in the MET plus MIC treated fetus liver tissue, whereas it arised in the MIC treated and MET treated fetus liver tissues reduced. A band at 1522 cm^{-1}, due to the stretching C=N and C=C, was not present in the control, MIC and MET treated fetus liver tissues, but was appeared in the MET plus MIC treated fetus liver tissue. A band at 2912 cm^{-1}, attributed to the stretching vibrations of CH2 and CH3 of phospholipids, cholesterol, and creatine, was appeared in the MET treated and MET plus MIC treated fetus liver tissues, but was not present in the control and MIC treated fetus liver tissues. A band at 2823 cm^{-1}, attributed to the stretching N-H (NH3+), was disappeared in the MIC treated and MET treated fetus liver tissues. A band at 2804 cm^{-1}, due to the stretching N-H (NH3+), was present in the control, but was disappeared in the other drug treated fetus liver tissue.

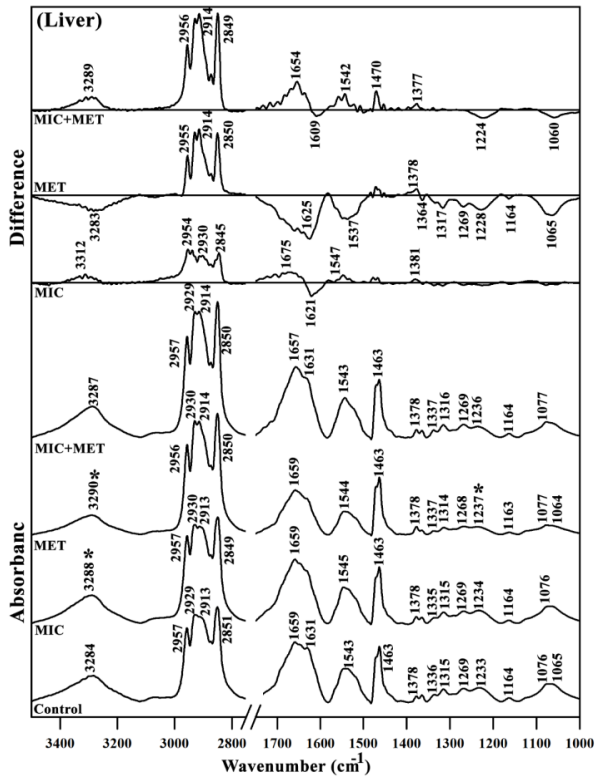

Figure 4. Mean FTIR spectra 2nd derivative of mentioned groups mice fetus liver tissue sections in the 2600–3700 cm^{-1} wavenumber region. Baseline correction and normalization were done for all the spectra with a reference to the band at 1545 cm^{-1} (amide II peak) for uniformity.

In the MIC treated and MET plus MIC treated fetus liver tissues, absorption at 1569 cm^{-1} (amide II), 1661 cm^{-1} (amide I), 1678 cm^{-1} (stretching C=O vibrations that are H-bonded), 1694 cm^{-1} (a high frequency vibration of an antiparallel β-sheet of amide I), and 1745 cm^{-1} (ester group (C=O) vibration of triglycerides)

increased, but in the MET treated fetus liver tissue reduced. In the MIC treated and MET treated fetus liver tissues, absorption at 1164 cm^{-1} (C-O stretching band of collagen (type I)), 1363 cm^{-1} (δ(CH2), ν (CC) (polysaccharides, pectin)), 1339 cm^{-1} (collagen), and 1316 cm^{-1} (amide III) reduced, but in the MET plus MIC treated fetus liver tissue increased . In the MIC treated and MET plus MIC treated fetus liver tissues, absorption at 1126 cm^{-1}, attributed to the ν(C-O), disaccharides, sucrose, ν(C-O) + ν(C-C), disaccharides, and sucrose increased, but in the MET treated fetus liver tissue remained unchanged. In the MIC treated and MET plus MIC treated fetus liver tissues, absorption at 1515 cm^{-1} (amide II) was unchanged, but in the MET treated fetus liver tissue reduced. Absorptions at 1079 cm^{-1} (ν_s $PO^{-}2$), 1058 cm^{-1} (stretching C-O deoxyribose), 1271 cm^{-1} (CHδ˙ rocking), and 1609 cm^{-1} (adenine vibration in DNA) reduced in all of them. A band at 1380 cm^{-1} (δCH3 stretching C-O, deformation C-H, and deformation N-H) increased in all the groups.

The bands in regions 2959 cm^{-1}, 2934 cm^{-1}, 2894 cm^{-1}, 2877 cm^{-1}, and 2849 cm^{-1}, mainly due to the stretching vibrations of CH2 and CH3 of phospholipids, cholesterol, and creatine, increased in all the groups.

3.3. FTIR quantitative analysis of the mice fetus liver tissues:

In order to make a quantitatively meaningful discrimination, three absorbance ratios of the peak heights between the control and the test groups at wavenumbers of 1124/1087, 1314/1234, and 1656/1634 cm^{-1} were measured. The statistical evaluations for the control and the drugs treated mice fetus liver tissues were shown in figures 6-8 as means plot and mean comparison

3.3.1. The absorbance ratio of 1124/1087

Absorbance in the region of 1124/1087 is totally related to the presence of PO^{-}_2 symmetric (phosphate II), ν (Co), ν (CC), and ring (polysaccharides, cellulose) groups. The mean values of the aforementioned ratio and the mean comparison plot for the different groups were observed in the figures 6-A and 6-B, respectively. Statistically significant differences were seen between all the groups ($p<0.01$).

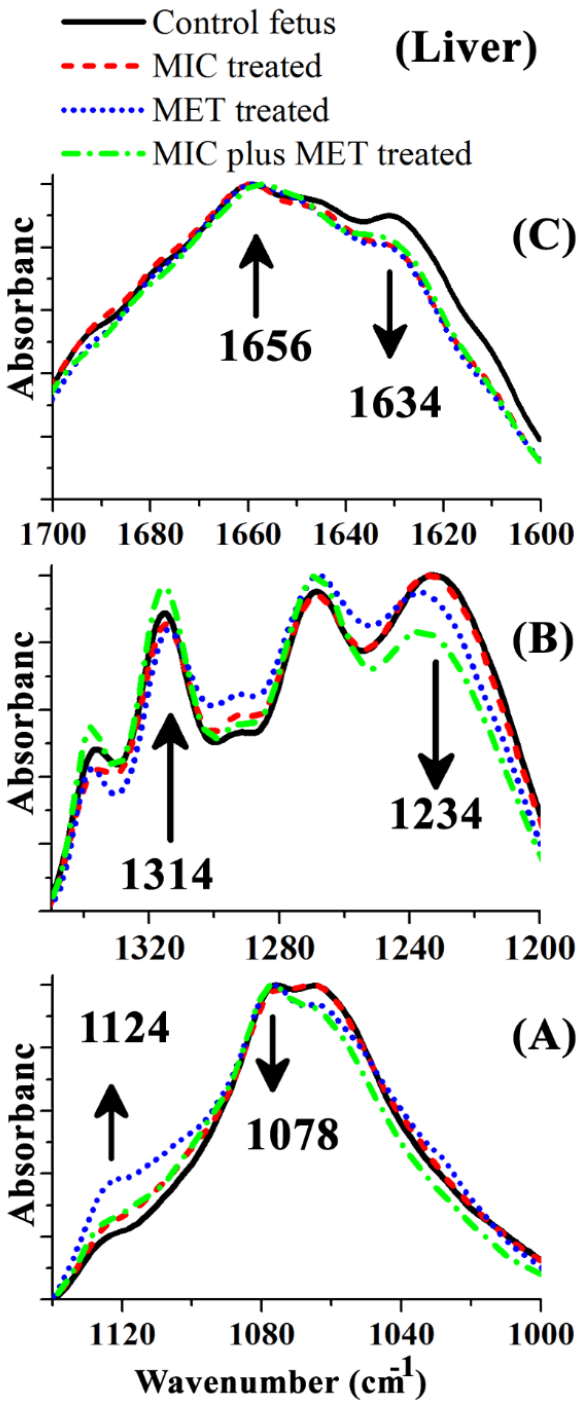

Figure 5. FTIR spectra of the control, MET, MIC and MET plus MIC groups mice fetus liver tissue sections in the various regions: 1000 to 1150 cm^{-1} (A), 1200 to1350 cm^{-1} (B), 1600 to 1700 cm^{-1} (C). To present the spectral variations each spectrum were normalized to the highest peak in specific regions for better visualization.

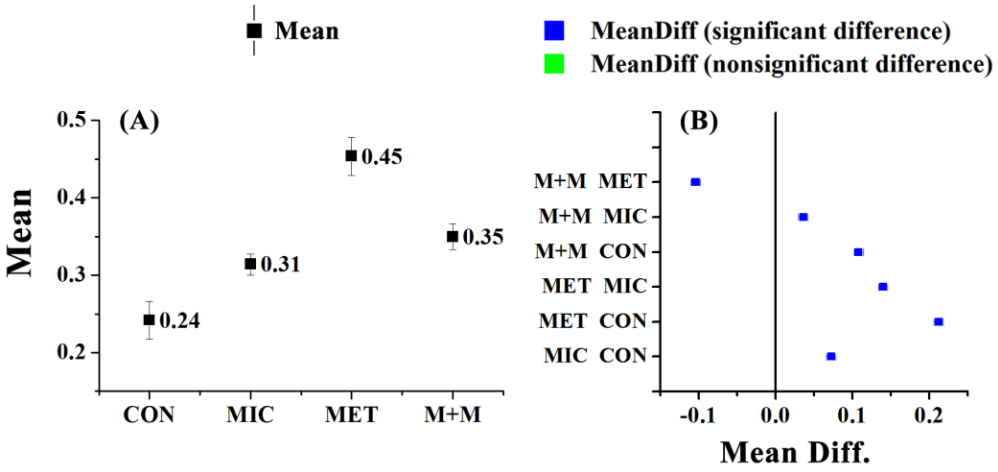

Figure. 6. Alterations in the ratios of 1124/1087 cm^{-1} (A) in the FTIR spectra of mouse fetus liver tissues. Results were presented as mean comparison plot; significant differences are marked in blue colors and non-significant differences are marked in green colors. One-way ANOVA followed by Tukey multiple comparisons were applied to analyze the data ($p < 0.01$). (For interpretation of the references to color in this figure legend, the reader is referred to the web version of this article.)

3.3.2. The absorbance ratio of 1314/1234

The absorbance ratio of 1314/1234 was applied for measuring the amide III band of proteins. Figures 7-A and 7-B show the mean values of this ratio and the mean comparison plot for the different groups, respectively. Clear separations were observed between the control and all the treated groups. Significant differences were seen between the control and MET plus MIC treated, MET treated and MIC treated, MIC treated and MET plus MIC treated mouse fetus liver tissues. There was not any significant difference between the MET treated and MIC treated mouse fetus liver tissues and those of the control group.

3.3.3. The absorbance ratio of 1656/1634

The ratio of the contents of amide I to C=C uracil and C=O in the fetus liver was presented by the absorbance ratio of 1656/1634. , The mean comparison plot, shown in figure 8-D, exhibited significant differences between the mouse fetus liver tissues of the control group and those of the MET treated, MIC treated, and MET plus MIC treated groups. There was not any significant difference between the means of the above mentioned ratio in the MET treated and MIC treated, MIC treated and MET plus MIC treated, and MET treated and MET plus MIC treated mouse fetus liver tissues.

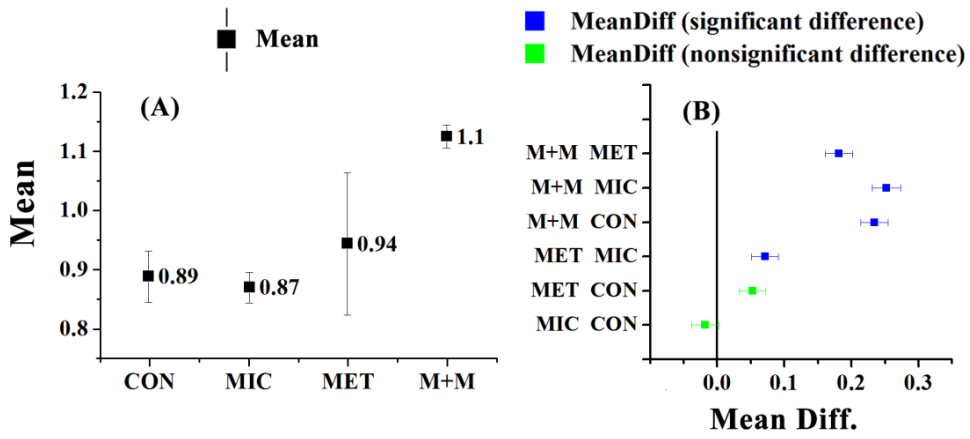

Figure. 7. Alterations in the ratios of 1314/1234 cm−1 (A), in the FTIR spectra of mouse fetus liver tissues. Means comparison plot applied for the results; significant and non-significant differences were displayed in blue and green colors, respectively. Data were analyzed by one-way ANOVA followed by Tukey multiple comparisons test ($p < 0.01$). (For interpretation of the references to color in this figure legend, the reader is referred to the web version of this article.)

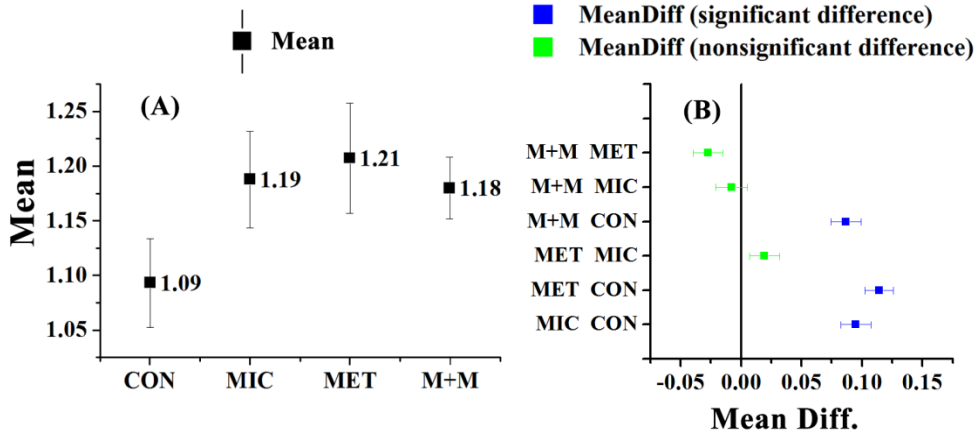

Figure. 8. Alterations in the ratios of 1656/1634 cm^{-1} in the FTIR spectra of mouse fetus liver tissues. Means comparison plot were used for the results; significant differences and non-significant differences were displayed in blue and green colors, respectively. Data are analyzed by one-way ANOVA followed by Tukey multiple comparisons test ($p < 0.01$). (For interpretation of the references to color in this figure legend, the reader is referred to the web version of this article.)

4. Conclusion

FTIR-MSP effectively is a powerful tool for biomedical research applications. During the past decades, biospectroscopy has proved to be capable of detecting the infra-structural abnormalities of the biological tissues like cancer. We reported new application of FTIR-MSP for recognition of molecular alterations in mice fetus tissues after exposure to Metronidazole, Miconazole, Levamisole, and Phenobarbital drugs in our previous researches [31, 39-41]. The potential of this method has been shown by detecting any degree of change in the fetus tissues even before any kind of morphological changes. However, any conclusion from a very complicated FTIR spectrum should be taken with caution, because of the complexity of the fetus matrix.

Azole drugs (such as Metronidazole, Miconazole, and etc.) have side effects on the phospholipids of cell membranes and can inhibit endogenous respiration and morphogenetic transformation of yeasts to the mycelial form. So in this study, we have tried to detect spectral changes of mouse fetus liver tissue after mother's exposure to concomitant use of MET and MIC as an example of FTIR- MSP application in teratology. Liver tissues of the fetuses treated with the above mentioned drugs and control group were compared using photomicrographs after staining with Haematoxylin and Eosin. The weight and the C-R length of the MET plus MIC treated mouse fetus were less than the other groups and there were some adverse effects for them due to their exposure to MET and MIC alone. As shown in the figures 3-5, MET and MIC alone and in combination have created some changes in all of the mice fetus liver biomolecules. These drugs induced some important alterations in the fetus liver proteins, nucleic acids, and fatty acids. There were significant differences of nucleic acid ratio between all the groups treated by MET and MIC (alone and in combination) (Figure 6), while there was significant difference of amid III ratio between the MET plus MIC treated group with the other groups and its production decreased, but there was not any significant difference between the MET treated and MIC treated mouse fetus liver tissues and those of the control group (Figure 7). The last figure (Figure 8) showed significant difference of amide I ratio between the MET plus MIC treated and control groups and its production increased.

FTIR biospectroscopy application in teratology is very challenging area, but it has been accepted as a reliable technique both for discovering the alterations and molecular mechanisms of fetus anomalies, caused by different agents; however, more investigations are required about its application.

Acknowledgment

This work was supported by the Pharmaceutical Sciences Research Center of Shahid Beheshti University of Medical Sciences.

Conflict of interest

There is no conflict of interest.

References

1. D.I. Edwards, Mechanisms of selective toxicity of metronidazole and other nitroimidazole drugs, The British journal of venereal diseases 56(5) (1980) 285-290.
2. J. Cantu, D. Garcia-Cruz, Midline facial defect as a teratogenic effect of metronidazole, Birth defects: original article series (1982).
3. A. Carvajal, A. Sánchez, G. Hurtarte, Metronidazole during pregnancy, International Journal of Gynecology & Obstetrics 48(3) (1995) 323-324.
4. A. Bendesky, D. Menéndez, P. Ostrosky-Wegman, Is metronidazole carcinogenic?, Mutation Research/Reviews in Mutation Research 511(2) (2002) 133-144.
5. C. Ito, Y. Shibutani, K. Inoue, K. Nakano, H. Ohnishi, Toxicological studies of miconazole. 2. Teratological studies of miconazole in rats, Iyakuhin Kenkyu 7 (1976) 367-376.
6. M. Engelen, M.d. Bock, J. Hare, L. Goossens, Effectiveness of an otic product containing miconazole, polymyxin B and prednisolone in the treatment of canine otitis externa: multi-site field trial in the US and Canada, International Journal of Applied Research in Veterinary Medicine 8(1) (2010) 21-30.
7. A.E. Czeizel, Z. Kazy, E. Puhó, Population-based case-control teratologic study of topical miconazole, Congenital Anom. 44(1) (2004) 41-45.
8. International Agency for Research on Cancer (IARC) - Summaries & Evaluations, METRONIDAZOLE (Group 2B), IPCS INCHEM, 1987, p. 250.
9. Metronidazole intravenous infusion. Metronidazole PI Amended 12 (2012).
10. H.T. Sørensen, H. Larsen, E.S. Jensen, A.M. Thulstrup, H.C. Schønheyder, G.L. Nielsen, A. Czeizel, E.S. Group, Safety of metronidazole during pregnancy: a cohort study of risk of congenital abnormalities, preterm delivery and low birth weight in 124 women, J. Antimicrob. Chemother. 44(6) (1999)
11. M. Chacko, S. Bhide, Carcinogenicity, perinatal carcinogenicity and teratogenicity of low dose metronidazole (MNZ) in Swiss mice, J. Cancer Res. Clin. Oncol. 112(2) (1986) 135-140.
12. F. Di Renzo, M.L. Broccia, E. Giavini, E. Menegola, Antifungal triazole derivative triadimefon induces ectopic maxillary cartilage by altering the morphogenesis of the first branchial arch, Birth Defects Research Part B: Developmental and Reproductive Toxicology 80(1) (2007) 2-11.
13. G.M. Tiboni, F. Marotta, A. Del Corso, F. Giampietro, Defining critical periods for itraconazole-induced cleft palate, limb defects and axial skeletal malformations in the mouse, Toxicol. Lett. 167(1) (2006) 8-18.
14. O. Diav-Citrin, S. Shechtman, T. Gotteiner, J. Arnon, A. Ornoy, Pregnancy outcome after gestational exposure to metronidazole: a prospective controlled cohort study, Teratology 63(5) (2001) 186-192.
15. T. Caro-Patón, A. Carvajal, I. Martín de Diego, L.H. Martín-Arias, A. Alvarez Requejo, E.R. Pinilla, Is metronidazole teratogenic? A meta-analysis, Br. J. Clin. Pharmacol. 44(2) (1997) 179-182.
16. P. Burtin, A. Taddio, O. Ariburnu, T.R. Einarson, G. Koren, Safety of metronidazole in pregnancy: a meta-analysis, Am. J. Obstet. Gynecol. 172(2) (1995) 525-529. DOI: 10.1016/0002-9378(95)90567-7
17. F. Greenberg, J.F. Reynolds, Possible metronidazole teratogenicity and clefting, American Journal of Medical Genetics Part A 22(4) (1985) 825-825.
18. Z. Kazy, E. Puhó, A.E. Czeizel, Teratogenic potential of vaginal metronidazole treatment during pregnancy, European Journal of Obstetrics & Gynecology and Reproductive Biology 123(2) (2005) 174-178.
19. G.M. Tiboni, F. Marotta, A.P. Castigliego, Teratogenic effects in mouse fetuses subjected to the concurrent in utero exposure to miconazole and metronidazole, Reprod. Toxicol. 26(3) (2008) 254-261.
20. M.J. Walsh, T.G. Fellous, A. Hammiche, W.R. Lin, N.J. Fullwood, O. Grude, F. Bahrami, J.M. Nicholson, M. Cotte, J. Susini, Fourier transform infrared microspectroscopy identifies symmetric PO2− modifications as a marker of the putative stem cell region of human intestinal crypts, Stem Cells 26(1) (2008) 108-118.
21. I.I. Patel, D.A. Shearer, S.W. Fogarty, N.J. Fullwood, L. Quaroni, F.L. Martin, J. Weisz, Infrared microspectroscopy identifies biomolecular changes associated with chronic oxidative stress in mammary epithelium and stroma of breast tissues from healthy young women: Implications for latent stages of breast carcinogenesis, Cancer Biol. Ther. 15(2) (2014) 225-235.
22. I.I. Patel, W.J. Harrison, J.G. Kerns, J. Filik, K. Wehbe, P.L. Carmichael, A.D. Scott, M.P. Philpott, M.D. Frogley, G. Cinque, Isolating stem cells in the inter-follicular epidermis employing synchrotron radiation-based Fourier-transform infrared microspectroscopy and focal plane array imaging, Anal. Bioanal. Chem. 404(6-7) (2012) 1745-1758.
23. J.G. Kelly, A.A. Ahmadzai, P. Hermansen, M.A. Pitt, Z. Saidan, P.L. Martin-Hirsch, F.L. Martin, A biospectroscopic interrogation of fine needle aspirates points towards segregation between graded categories: an initial study towards diagnostic screening, Anal. Bioanal. Chem. 401(3) (2011) 957-967.
24. Z. Movasaghi, S. Rehman, D.I. ur Rehman, Fourier transform infrared (FTIR) spectroscopy of biological tissues, Appl. Spectrosc. Rev. 43(2) (2008) 134-179.
25. E. Bogomolny, M. Huleihel, Y. Suproun, R.K. Sahu, S. Mordechai, Early spectral changes of cellular malignant transformation using Fourier transform infrared microspectroscopy, J. Biomed. Opt. 12(2) (2007) 024003-024003-9.
26. M.J. Baker, J. Trevisan, P. Bassan, R. Bhargava, H.J. Butler, K.M. Dorling, P.R. Fielden, S.W. Fogarty, N.J. Fullwood, K.A. Heys, Using Fourier transform IR spectroscopy to analyze biological materials, Nat. Protoc. 9(8) (2014) 1771-1791.
27. M. Miljković, B. Bird, K. Lenau, A.I. Mazur, M. Diem, Spectral Cytopathology: new aspects of data collection, manipulation and confounding effects, Analyst 138(14) (2013) 3975-3982.
28. P. Bassan, A. Sachdeva, J. Lee, P. Gardner, Substrate contributions in micro-ATR of thin samples: implications for analysis of cells, tissue and biological fluids, Analyst 138(14) (2013) 4139-4146.
29. V. Zohdi, D.R. Whelan, B.R. Wood, J.T. Pearson, K.R. Bambery, M.J. Black, Importance of tissue preparation methods in FTIR micro-spectroscopical analysis of biological tissues:'Traps for new users', PLoS One 10(2) (2015) e0116491.
30. R. Bhargava, D.C. Fernandez, S.M. Hewitt, I.W. Levin, High throughput assessment of cells and tissues: Bayesian classification of spectral metrics from infrared vibrational spectroscopic imaging data, Biochim Biophys Acta Biomembr 1758(7) (2006) 830-845.
31. A. Ashtarinezhad, F.H. Shirazi, H. Vatanpour, B. Mohamazadehasl, A. Panahyab, M. Nakhjavani, FTIR-Microspectroscopy detection of Metronidazole teratogenic effects on mice fetus, Iran J Pharm Res 13(Suppl) (2014) 101.
32. S. Olsztyńska-Janus, K. Szymborska-Małek, M. Gąsior-Głogowska, T. Walski, M. Komorowska, W. Witkiewicz, C. Pezowicz, M. Kobielarz, S. Szotek, Spectroscopic techniques in the study of human tissues and their components. Part I: IR spectroscopy, Acta Bioeng Biomech 14 (2012) 101-115.

33. F. Sullivan, P. McElhatton, Teratogenic acitivity of the antiepileptic drugs phenobarbital, phenytoin, and primidone in mice, Toxicol. Appl. Pharmacol. 34(2) (1975) 271-282.
34. D.F. Bishop, A. Johansson, R. Phelps, A.A. Shady, M.C. Ramirez, M. Yasuda, A. Caro, R.J. Desnick, Uroporphyrinogen III synthase knock-in mice have the human congenital erythropoietic porphyria phenotype, including the characteristic light-induced cutaneous lesions, The American Journal of Human Genetics 78(4) (2006) 645-658.
35.N. Böhm, N. Noltemeyer, Excessive reversible phenobarbital induced nuclear DNA-polyploidization in the growing mouse liver, Histochemistry 72(1) (1981) 63-74.
36. M.K. Mahabady, R. Ranjbar, A. Arzi, A. Papahn, H. Najafzadeh, A comparison study of effects of Echinacea extract and levamisole on phenytoin-induced cleft palate in mice, Regul. Toxicol. Pharmacol. 46(3) (2006) 163-166.
37. G. Avwioro, Histochemical uses of haematoxylin—a review, JPCS 1 (2011) 24-34.
38. I.o.L.A.R.C.o. Care, U.o.L. Animals, N.I.o.H.D.o.R. Resources, Guide for the care and use of laboratory animals, National Academies1985.
39. A. Ashtarinezhad, A. Panahyab, B. Mohamadzadeh asl, H. Vatanpour, F. H. Shirazi, FTIR Determination of Miconazole Effects on Mice Fetus Brain Tissue, Iranian Journal of Pharmaceutical Sciences 10(2) (2015) 79-84.
40. A. Ashtarinezhad, A. Panahyab, B. Mohamadzadehasl, H. Vatanpour, F.H. Shirazi, FTIR Microspectroscopy Reveals Chemical Changes in Mice Fetus Following Phenobarbital Administration, Iranian journal of pharmaceutical research: IJPR 14(Suppl) (2015) 121.
41. A. Ashtarinezhad, A. Panahyab, S. Shaterzadeh-Oskouei, H. Khoshniat, B. Mohamadzadehasl, F.H. Shirazi, Teratogenic study of phenobarbital and levamisole on mouse fetus liver tissue using biospectroscopy, J. Pharm. Biomed. Anal. 128 (2016) 174-183.